Simulating the solar wind acceleration throughout the solar cycle

Rui Pinto, Alexis Rouillard

with the kind help from a whole bunch of other people:
Sacha Brun (CEA Saclay, AIM/SAp), Laurène Jouve (IRAP, Toulouse), Sean Matt (U. Exeter)
Roland Grappin (LPP, École Polytechnique), Yi-Ming Wang (NRL)
Andrea Verdini (ROB, Brussels), Marco Velli (JPL & Firenze)

The solar wind and the solar cycle

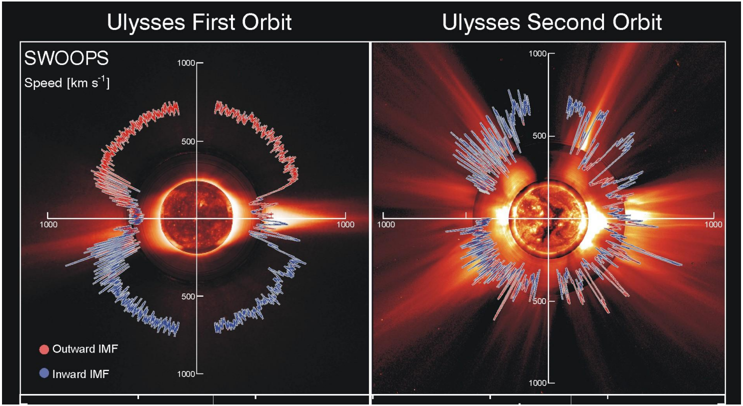

McComas et al. (2003)

Solar minimum

Fast wind / slow wind separation
Dipolar large-scale magnetic field, **few AR**

Solar maximum

Fast wind / slow wind mixed together
Multipolar large-scale magnetic field, **many AR**

Fast/slow wind: summary

Fast wind

- Faster flow **(450 – 800 km/s)**, **lower mass flux**
- Temperature: lower T_{max}, higher T (1 AU)
- **Confined to coronal holes**
- **Fluctuations detected: small amplitude, wave turbulence**
- Heavy-ion composition: mostly low *freeze-in* T

Slow wind

- Slower flow **(200 – 450 km/s)**, **higher mass flux**
- Temperature: higher T_{max}, lower T (1 AU)
- **Coronal hole boundaries, streamer tops, maybe also active regions**
- **Fluctuations: high amplitude; waves**, blobs, maybe helical structures
- Heavy-ion composition: closed corona *freeze-in* T

Key questions:

1. What cause the fast/slow wind segregation?
2. What are the consequences for the heliosphere?

Models

STELEM (kinematic dynamo)

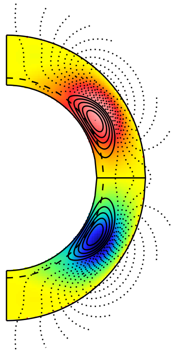

- Convective zone, tachocline
- Meridional circulation, diff. rotation
- Surface fields ("butterfly diagram")

(Jouve and Brun, 2007)

DIP (corona, solar wind)

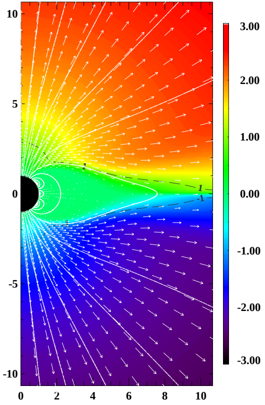

- Isothermal corona and wind
- Self-consistent time-dependent mass flux at the boundaries

(Grappin et al., 2000; Pinto et al., 2010)

Dynamo – solar wind; 1 solar cycle

(Pinto et al., 2011)

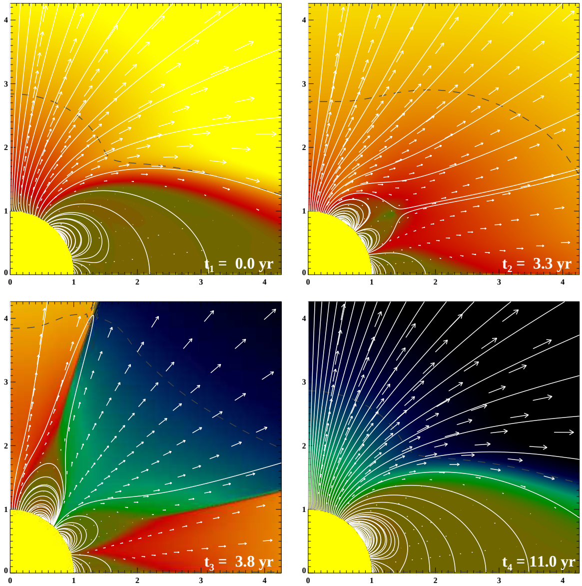

Wind speed during the cycle

Simulation (11 years, 15 $R_\odot$)

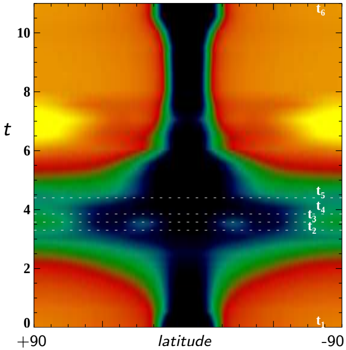

IPS radio maps (1997-2009, 1 AU)

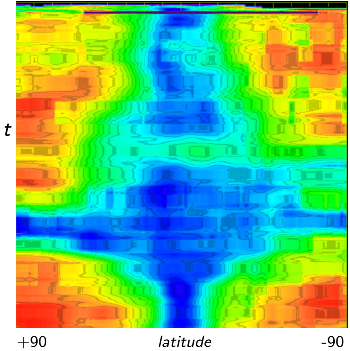

Time-latitude diagrams,
fast wind; slow wind

(Shibasaki, K.; *priv. comm.*)
(see also: Manoharan, 2012; Tokumaru et al., 2010)

Wind speed during the cycle

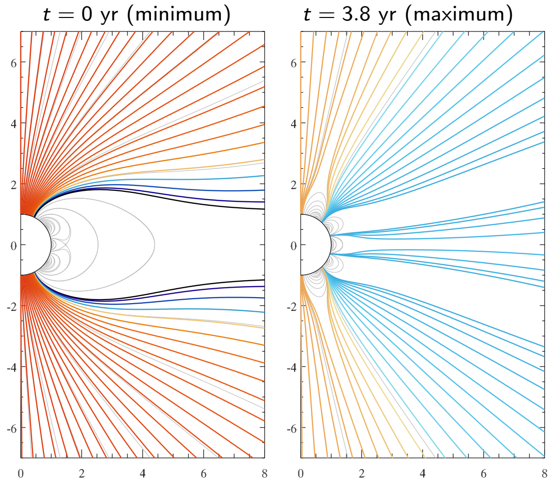

Magnetic field lines coloured according to terminal wind speed.

2 instants of the cycle, $r = 1 - 8\ R_\odot$

Magnetic field geometry
vs.
terminal wind speed

Strongly expanding flux-tubes

⇓

Slow wind

cf. WSA semi-empirical relation
(Arge and Pizzo, 2000; Wang and Sheeley, 1990)

But **transition to slow wind is sharper**.

Dark red - orange: fast wind flow
Dark blue - cyan: slow wind flow
(Pinto, Rouillard, Wang, et al, *in prep.*)

Wind speed during the cycle

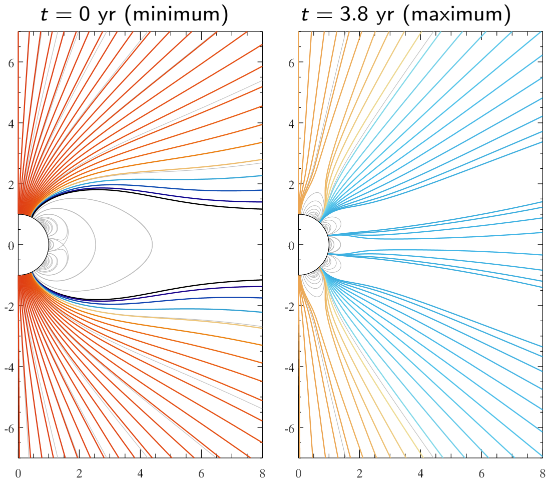

Magnetic field lines coloured according to terminal wind speed.

2 instants of the cycle, $r = 1 - 8\ R_\odot$

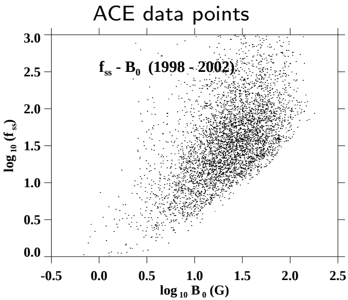

(Wang, *priv. comm.*; also Wang, 2012)

Dark red - orange: fast wind flow
Dark blue - cyan: slow wind flow
(Pinto, Rouillard, Wang, et al, *in prep.*)

Wind speed during the cycle

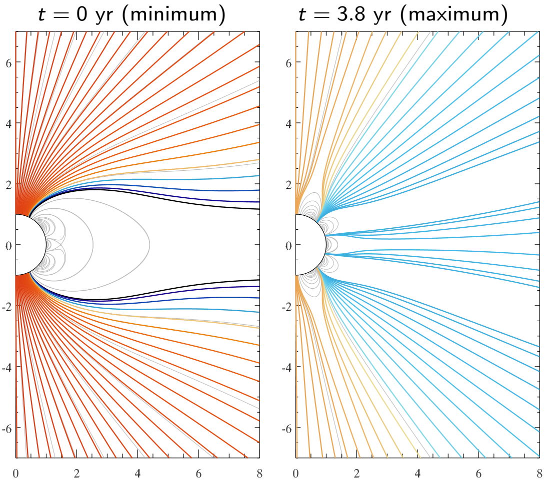

Magnetic field lines coloured according to terminal wind speed.

2 instants of the cycle, $r = 1 - 8\ R_\odot$

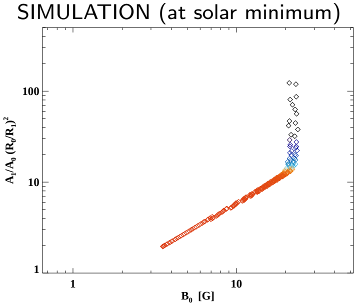

Dark red - orange: fast wind flow
Dark blue - cyan: slow wind flow
(Pinto, Rouillard, Wang, et al, *in prep.*)

Wind speed during the cycle

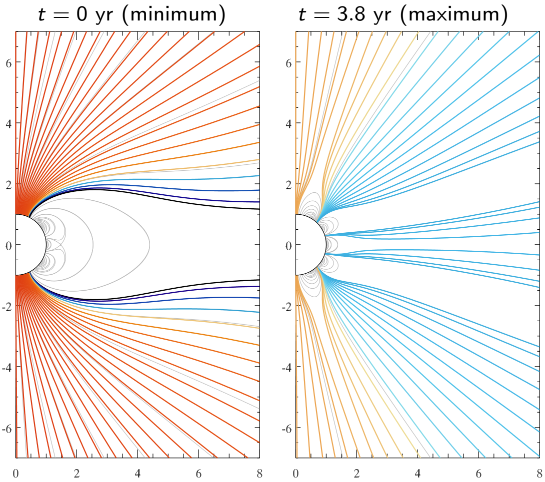

Magnetic field lines coloured according to terminal wind speed.

2 instants of the cycle, $r = 1 - 8\ R_\odot$

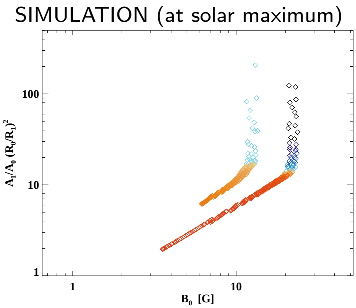

Dark red - orange: fast wind flow
Dark blue - cyan: slow wind flow
(Pinto, Rouillard, Wang, et al, *in prep.*)

Wind speed during the cycle

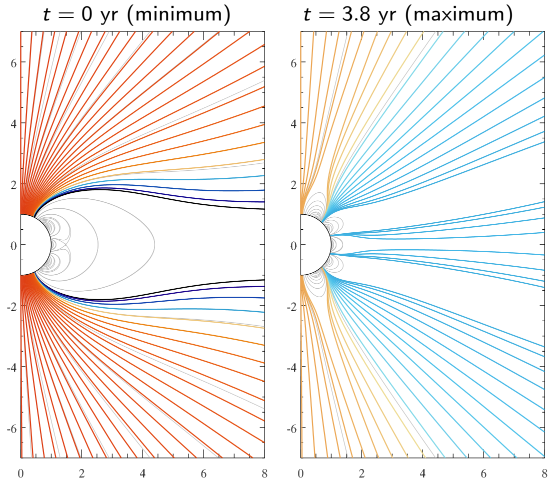

Magnetic field lines coloured according to terminal wind speed.

2 instants of the cycle, $r = 1 - 8\ R_\odot$

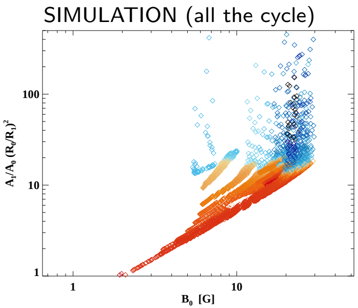

Sharp transition bw. fast/slow wind.

Lower cut-off: least multipolar field

Strong correlation bw. f and V_r

Dark red - orange: fast wind flow
Dark blue - cyan: slow wind flow
(Pinto, Rouillard, Wang, et al, *in prep.*)

Expansion and radial velocity, latitudinal profiles

Minimum

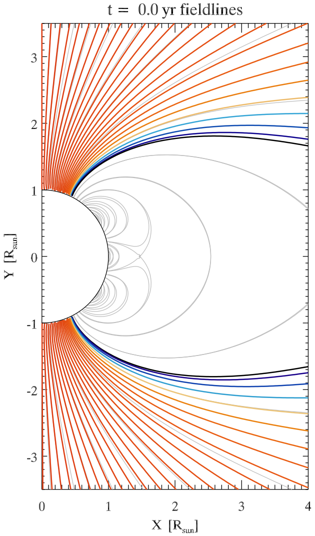

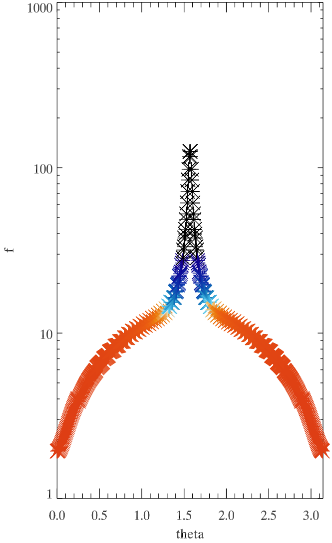

Expansion and radial velocity, latitudinal profiles

Maximum

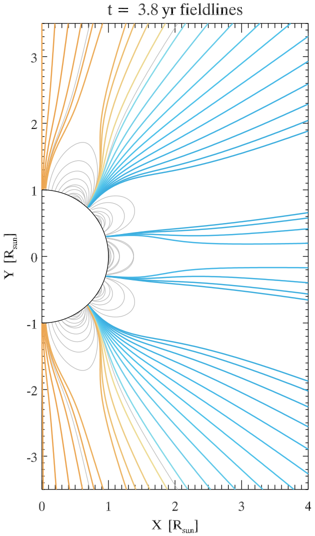

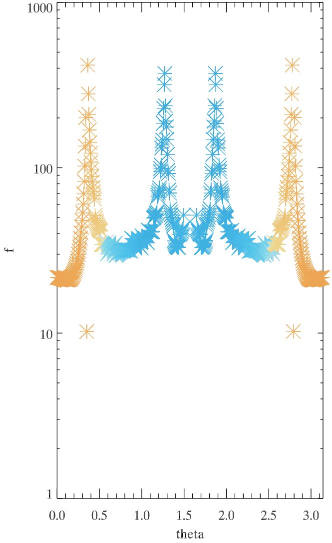

Field-line inclination

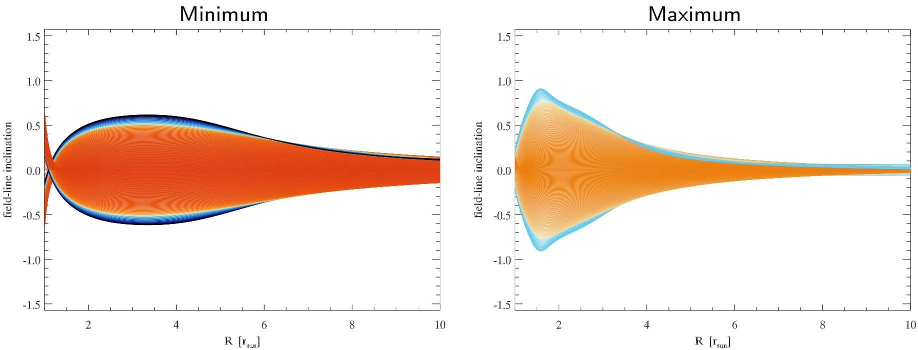

→ field-line inclination between 1.5 – 4 $R_\odot$ has an effect on wind speed (*where the wind flow acceleration is maximal*)

(Pinto, Rouillard, Wang, et al, *in prep.*,
see also Li, et al., 2011, Lionello, et al., 2014)

Differential rotation in the corona

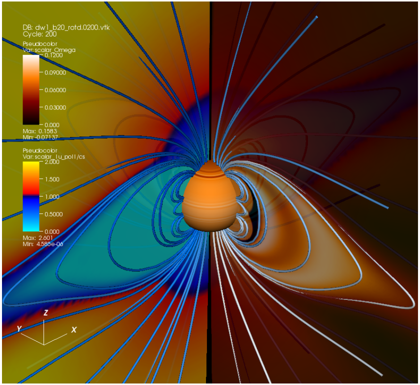

$t_1 = 0$ yr

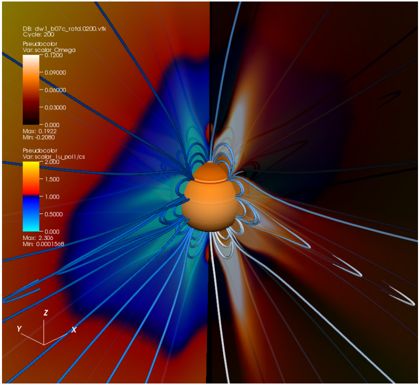

$t_4 = 3.8$ yr

blue: wind speed v_r/c_s; orange:rotation rate Ω

Surface differential rotation profile:
$\Omega(\theta) = \Omega_a + \Omega_b \sin^2\theta + \Omega_c \sin^4\theta$
(Snodgrass and Ulrich, 1990)

Shear and vorticity generated at
streamer / coronal hole boundaries
(maybe plasma exchange?)

(Grappin et al., 2008; Pinto et al., 2013)

Alfvén radius

Alfvén surface

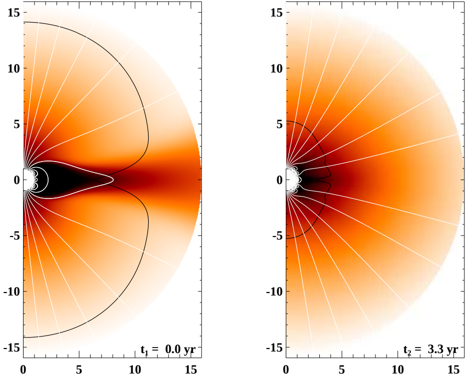

Average Alfvén radius $\langle r_A \rangle$

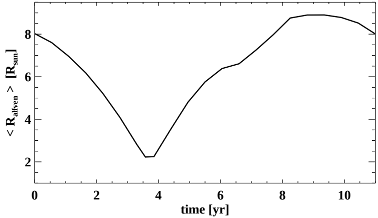

$$\langle r_A \rangle = 2 - 9 \; R_\odot$$

Consequences:
Solar wind properties below/above Alfvén surface (fluctuations, turbulence; Solar Probe+)
(Verdini, Grappin, Pinto, and Velli, 2012)

Efficiency of ang. momentum transport $\propto \langle r_A \rangle^2$
(Weber and Davis, 1967)

Predicting the terminal wind speed and inputs for ENLIL

WSA semi-empirical scaling law

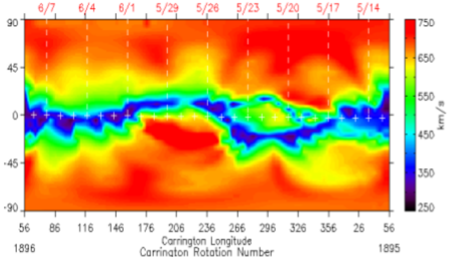

$$V_{wind} = 265 + \frac{1.5}{(1+f_{ss})^{1/3}} \times$$
$$\times \left[5.8 - 1.6 \exp\left[1 - \frac{{\theta_b}^3}{7.5^3}\right]\right]^{3.5} \text{ km s}^{-1}$$

f_{ss}: total flux-tube expansion ratio (Wang, 1995; Velli 2013)
θ_b: distance to coronal hole boundary

Predicting the terminal wind speed and inputs for ENLIL

WSA semi-empirical scaling law

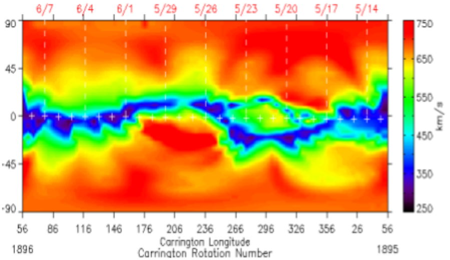

$$V_{wind} = 265 + \frac{1.5}{(1+f_{ss})^{1/3}} \times$$
$$\times \left[5.8 - 1.6 \exp\left[1 - \frac{{\theta_b}^3}{7.5^3}\right]\right]^{3.5} \text{ km s}^{-1}$$

f_{ss}: total flux-tube expansion ratio (Wang, 1995; Velli 2013)
θ_b: distance to coronal hole boundary

Going beyond WSA

→ Substitute θ_b by more physical terms

→ Wind speed at **different heights**

→ **Other plasma parameters** (density, temperature, etc)

→ Add *minimal* amount of complexity

New strategy

Multi-VP

Multiple 1D flux-tube wind solutions sampling the whole corona.

(Mid-way between specialised local models and global 3D MHD models)

Multi-VP strategy

Sun / surface observations
(magnetograms)
↓
Coronal B-field reconstruction
(PFSS SolarSoft)
↓
MULTI-VP
↓
Heliospheric propagation models
(ENLIL)
↓
Earth / interplanetary medium
In-situ data, heliospheric imaging

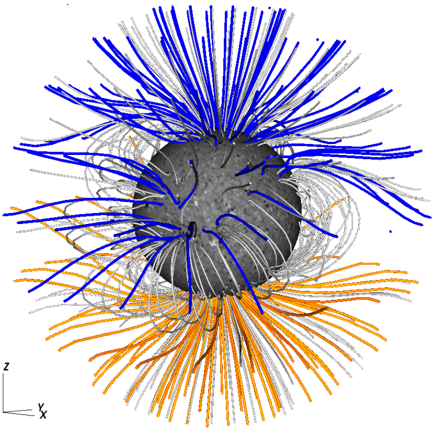

Surface magnetic field B_r (± 30 G)
PFSS field lines positive/negative polarity

Multi-VP strategy

Sun / surface observations
(magnetograms)
↓

Coronal B-field reconstruction
(PFSS SolarSoft)

↓

MULTI-VP

↓

Heliospheric propagation models
(ENLIL)

↓

Earth / interplanetary medium
In-situ data, heliospheric imaging

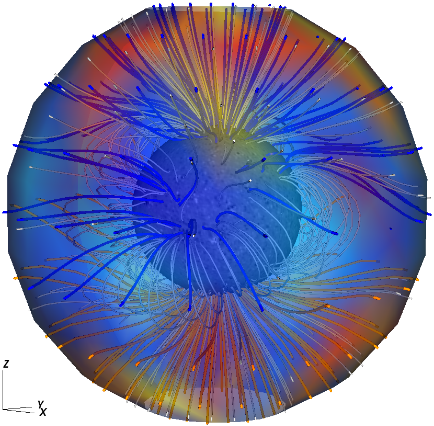

Wind speed: red = 650 km/s; blue = 350 km/s

Multi-VP strategy

Sun / surface observations
(magnetograms)

↓

Coronal B-field reconstruction
(PFSS SolarSoft)

↓

MULTI-VP

↓

Heliospheric propagation models
(ENLIL)

↓

Earth / interplanetary medium
In-situ data, heliospheric imaging

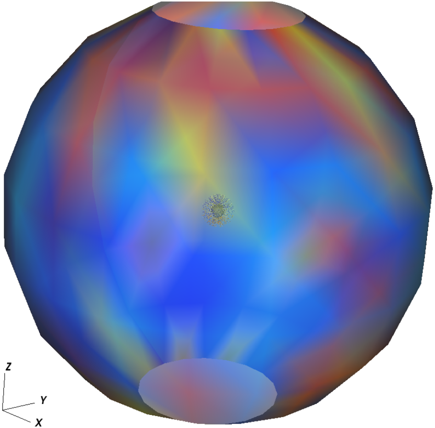

Wind speed: red = 650 km/s; blue = 350 km/s

Wind flows surface to heliosphere

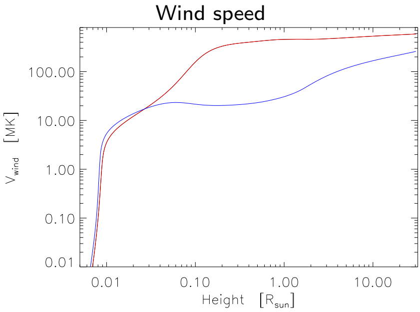

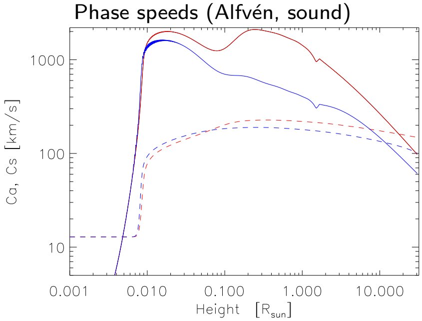

Red lines: fast wind profile
Blue lines: slow wind profile

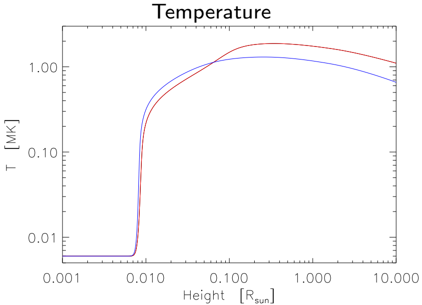

Summary

- **Variations of global magnetic topology of the corona** have a **major effect** on the **wind properties**.
  Simple geometrical parameters seem to control the wind speed; alternative to WSA?

- **Coronal rotation** structured by global magnetic field
  Sources of shear/vorticity in the corona (i.e, not foot-point forcing)

- **MULTI-VP**: new global wind model ($1 - 32\ R_\odot$)
  Fast model, chromospheric and coronal stratification.
  Wind speeds, densities, temperatures, phase speeds, etc.

- **HELCATS**: synoptic maps of wind speed at $\sim 20\ R_\odot$ (inputs for ENLIL)

- Dynamical events (propagation of disturbances)

- **Solar data** (surface and corona mag. fields, IPS radio)

References I

C. N. Arge and V. J. Pizzo. Improvement in the prediction of solar wind conditions using near-real time solar magnetic field updates. *Journal of Geophysical Research*, 105:10465–10480, May 2000. URL http://adsabs.harvard.edu/abs/2000JGR...10510465A.

G. Barnes, A. C. Birch, K. D. Leka, and D. C. Braun. Helioseismology of Pre-emerging Active Regions. III. Statistical Analysis. *The Astrophysical Journal*, 786:19, 2014. ISSN 0004-637X. doi: 10.1088/0004-637X/786/1/19. URL http://cdsads.u-strasbg.fr/abs/2014ApJ...786...19B.

Allan Sacha Brun and Juri Toomre. Turbulent Convection under the Influence of Rotation: Sustaining a Strong Differential Rotation. *The Astrophysical Journal*, 570(2):865–885, 2002. ISSN 0004-637X. URL http://www.iop.org/EJ/abstract/0004-637X/570/2/865/.

Allan Sacha Brun, Mark S. Miesch, and Juri Toomre. Global-Scale Turbulent Convection and Magnetic Dynamo Action in the Solar Envelope. *Astrophysical Journal*, 614:1073–1098, October 2004. URL http://adsabs.harvard.edu/abs/2004ApJ...614.1073B.

T. C. Clune, J. R. Elliott, M. S. Miesch, J. Toomre, and G. A. Glatzmaier. Computational aspects of a code to study rotating turbulent convection in spherical shells. *Parallel Computing*, 25(4):361–380, April 1999. ISSN 0167-8191. doi: 10.1016/S0167-8191(99)00009-5. URL http://www.sciencedirect.com/science/article/B6V12-48CP9S8-F/2/152989a83d20197c845eecf012f5e06c.

S. R. Cranmer. Winds of Main-Sequence Stars: Observational Limits and a Path to Theoretical Prediction. volume 384, page 317, April 2008. URL http://adsabs.harvard.edu/abs/2008ASPC..384..317C.

C. E. Deforest and J. B. Gurman. Observation of Quasi-periodic Compressive Waves in Solar Polar Plumes. *Astrophysical Journal*, 501:L217, July 1998. URL http://adsabs.harvard.edu/abs/1998ApJ...501L.217D.

R. Grappin, J. Léorat, and A. Buttighoffer. Alfvén wave propagation in the high solar corona. *Astronomy and Astrophysics*, 362: 342–358, October 2000. URL http://adsabs.harvard.edu/abs/2000A%26A...362..342G.

R. Grappin, G. Aulanier, and R. Pinto. The MHD coupling between coronal dynamics and photospheric motions. *Astronomy and Astrophysics*, 490:353–356, October 2008. URL http://adsabs.harvard.edu/abs/2008A%26A...490..353G.

R. Grappin, J. Léorat, S. Leygnac, and R. Pinto. Search for a self-consistent solar wind model. *Twelfth International Solar Wind Conference*, 1216:24–27, March 2010. URL http://adsabs.harvard.edu/abs/2010AIPC.1216...24G.

L. Jouve and A. S. Brun. On the role of meridional flows in flux transport dynamo models. *Astronomy and Astrophysics*, 474: 239–250, October 2007. URL http://adsabs.harvard.edu/abs/2007A%26A...474..239J.

References II

Laurène Jouve and Allan Sacha Brun. Three-Dimensional Nonlinear Evolution of a Magnetic Flux Tube in a Spherical Shell: Influence of Turbulent Convection and Associated Mean Flows. *Astrophysical Journal*, 701:1300–1322, August 2009. URL `http://adsabs.harvard.edu/abs/2009ApJ...701.1300J`.

P. K. Manoharan. Three-dimensional Evolution of Solar Wind during Solar Cycles 22-24. *The Astrophysical Journal*, 751:128, June 2012. ISSN 0004-637X. doi: 10.1088/0004-637X/751/2/128;. URL `http://adsabs.harvard.edu/abs/2012ApJ...751..128M`.

D. J. McComas, H. A. Elliott, N. A. Schwadron, J. T. Gosling, R. M. Skoug, and B. E. Goldstein. The three-dimensional solar wind around solar maximum. *Geophysical Research Letters*, 30:24–1, 2003. URL `http://adsabs.harvard.edu/abs/2003GeoRL..30j..24M`.

Scott W. McIntosh, Robert J. Leamon, Joseph B. Gurman, Jean-Philippe Olive, Jonathan W. Cirtain, David H. Hathaway, Joan Burkepile, Mark Miesch, Robert S. Markel, and Leonard Sitongia. Hemispheric Asymmetries of Solar Photospheric Magnetism: Radiative, Particulate, and Heliospheric Impacts. *The Astrophysical Journal*, 765:146, March 2013. ISSN 0004-637X. doi: 10.1088/0004-637X/765/2/146. URL `http://adsabs.harvard.edu/abs/2013ApJ...765..146M`.

R. Pinto, R. Grappin, Y.-M. Wang, and J. Léorat. Time-dependent hydrodynamical simulations of slow solar wind, coronal inflows, and polar plumes. *Astronomy and Astrophysics*, 497:537–543, 2009. URL `http://adsabs.harvard.edu/abs/2009A%26A...497..537P`.

R. Pinto, R. Grappin, and J. Leorat. Coronal Inflows and Giant Polar Plumes. In *Twelfth International Solar Wind Conference*, volume 1216, pages 80–83, Saint-Malo, (France), March 2010. AIP. doi: 10.1063/1.3395968. URL `http://link.aip.org/link/?APC/1216/80/1`.

R. F. Pinto, R. Grappin, M. Velli, and A. Verdini. Coupling the solar surface and the corona: Coronal rotation, Alfvén wave-driven polar plumes. volume 1539, pages 58–61, June 2013. ISBN 0094-243X. doi: 10.1063/1.4810989;. URL `http://adsabs.harvard.edu/abs/2013AIPC.1539...58P`.

Victor Réville, Allan Sacha Brun, Sean P. Matt, Antoine Strugarek, and Rui F. Pinto. The Effect of Magnetic Topology on Thermally Driven Wind: Toward a General Formulation of the Braking Law. *The Astrophysical Journal*, 798:116, January 2015. ISSN 0004-637X. doi: 10.1088/0004-637X/798/2/116. URL `http://adsabs.harvard.edu/abs/2015ApJ...798..116R`.

Herschel B. Snodgrass and Roger K. Ulrich. Rotation of Doppler features in the solar photosphere. *The Astrophysical Journal*, 351: 309, March 1990. ISSN 0004-637X, 1538-4357. doi: 10.1086/168467. URL `http://adsabs.harvard.edu/doi/10.1086/168467`.

References III

Munetoshi Tokumaru, Masayoshi Kojima, and Ken'ichi Fujiki. Solar cycle evolution of the solar wind speed distribution from 1985 to 2008. *Journal of Geophysical Research (Space Physics)*, 115:04102, April 2010. URL http://adsabs.harvard.edu/abs/2010JGRA..11504102T.

S. Toriumi and T. Yokoyama. Three-dimensional magnetohydrodynamic simulation of the solar magnetic flux emergence. Parametric study on the horizontal divergent flow. *Astronomy and Astrophysics*, 553:55, 2013. ISSN 0004-6361. doi: 10.1051/0004-6361/201321098;. URL http://adsabs.harvard.edu/abs/2013A%26A...553A..55T.

Andrea Verdini, Roland Grappin, Rui Pinto, and Marco Velli. On the Origin of the 1/f Spectrum in the Solar Wind Magnetic Field. *The Astrophysical Journal Letters*, 750:L33, May 2012. URL http://adsabs.harvard.edu/abs/2012ApJ...750L..33V.

Y.-M. Wang. Cyclic Magnetic Variations of the Sun. volume 154, page 131, 1998. URL http://adsabs.harvard.edu/abs/1998ASPC..154..131W.

Y.-M. Wang and N. R. Sheeley. Solar wind speed and coronal flux-tube expansion. *Astrophysical Journal*, 355:726–732, June 1990. URL http://adsabs.harvard.edu/abs/1990ApJ...355..726W.

Y.-M. Wang and N. R. Sheeley. Sources of the Solar Wind at Ulysses during 1990-2006. *Astrophysical Journal*, 653:708–718, December 2006. URL http://adsabs.harvard.edu/abs/2006ApJ...653..708W.

Edmund J. Weber and Leverett Davis. The Angular Momentum of the Solar Wind. *Astrophysical Journal*, 148:217, April 1967. URL http://adsabs.harvard.edu/abs/1967ApJ...148..217W.

Multi-1D approach

$$\partial_t \rho + \nabla \cdot (\rho \mathrm{u}) = 0$$

$$\partial_t \mathrm{u} + (\mathrm{u} \cdot \nabla)\, \mathrm{u} = -\frac{\nabla (P + P_w)}{\rho} - \frac{GM}{r^2}\hat{\mathrm{r}} + \nu \nabla^2 u$$

$$\partial_t T + \mathrm{u} \cdot \nabla T + (\gamma - 1)\, T \nabla \cdot \mathrm{u} = - \frac{\gamma - 1}{\rho}\left[\nabla \cdot F_h + \nabla \cdot F_c + \rho^2 \Lambda (T)\right]$$

(F_h: external heat flux;
F_c: SH conductive flux, transition to ballistic flux)
Ideal e-o-s with $\gamma = 5/3$

Magnetic field inclination:
$\Rightarrow$ $-g_0 \cos\alpha$, $\nabla P \cos\alpha$, heat fluxes $//\mathbf{B}$

(*cf.* Li, et al., 2011, Lionello, et al., 2014)

Divergence operator:

$$\nabla \cdot (*) = \frac{1}{A(r)} \frac{\partial}{\partial r} (A(r) *) = B \frac{\partial}{\partial r}\left(\frac{*}{B}\right)$$

(Grappin et al., 2010; Pinto et al., 2009; Verdini et al., 2012)

Standard phenomenological heating flux:

$$F_h = F_{p0} \left(\frac{A_0}{A}\right)^{(-1)} \exp\left[-\frac{r - R_\odot}{H_p}\right]$$

where $\left(\frac{A_0}{A}\right)^{(-1)} = \left(\frac{B}{B_0}\right)$, and $H_p \sim 1 \;\; \mathrm{R}_\odot$.

Other forms, Alfvèn wave dissipation:

$$F_h = F_{b0} \left(\frac{A_0}{A}\right) \left(\frac{B}{B_0}\right)^{\mu - 1} = F_{b0} \left(\frac{B}{B_0}\right)^{\mu}$$

where, typically, $\mu - 1 = 1/2$.

$$F_w = F_{w0} * \text{WKB operator}$$

Localised heating (emulating, e.g, transient ohmic dissipation):

$$F_r \propto erf(r_0, \delta r) \Rightarrow \nabla \cdot F_r = F_{r0} e^{-\frac{(r - r_0)^2}{\delta r^2}}$$

Reference surface flux:
$F_0 = 4 - 8 \times 10^5 \ \mathrm{erg} \cdot \mathrm{cm}^{-2}\mathrm{s}^{-1}$

Key parameters

1) Super-radial expansion
Fast to moderately slow winds
(fast/slow wind not sharp enough,
slow wind not slow enough)

2) Field-line inclination
around coronal streamers
(makes the slow wind slower, by ∼ 15%)

3) Appropriate heating functions
(how much energy, where it's dissipated)

Effect of inclination on wind speed (Pinto, Rouillard, et al, in prep.)

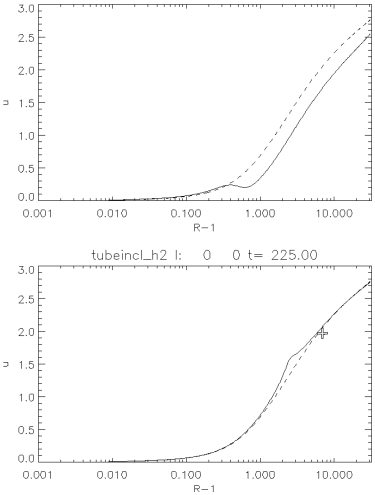

Coronal rotation

Partial chromospheric reflection; partial foot-point leakage

$$\delta L_a^+ = (1+a)\, f(t) - a\delta L_a^- \,,$$

$$a = \frac{1-\epsilon}{1+\epsilon}, \quad \epsilon = \frac{C_A^{photosphere}}{C_A^{corona}} \,.$$

$\delta L_a^\pm$: forces and torques applied at the surface from above and below

(*cf.* Pinto, Verdini, et al., 2012)

$\epsilon = 1$ "fully-transparent"

$\epsilon \to 0$ line-tied approximation. Valid for $\delta t \lesssim \tau_A$. (Grappin, Aulanier, Pinto, 2008)

$\epsilon = 0.01$ canonic value.

Why?

- **Consistency of mass and momentum fluxes at the boundary**
- Sustain the coronal rotation against the solar wind magnetic breaking torque, while still allowing for the necessary amount of footpoint leakage (coronal stress build-up and release, cf. Jardine et. al 2013).
- Allow for **time-dependent surface perturbations**
- Avoid the chromosphere ("slow perturbations")

Mass loss rate $\dot{M}\,[M_\odot/yr]$

SIMULATION

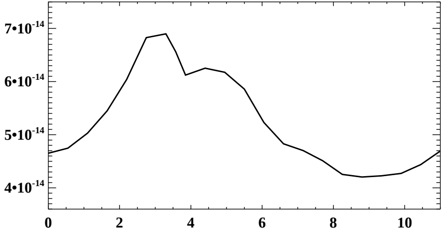

time (11 years, **1 cycle***)*

(Cranmer, 2008; Wang, 1998)

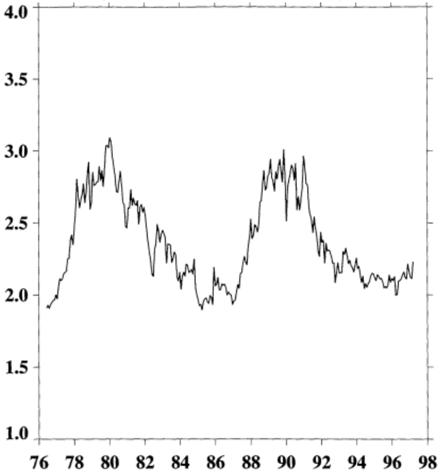

time (22 years, **2 cycles***)*

$\max\left(\dot{M}\right) / \min\left(\dot{M}\right) \approx 1.6$

$\langle \dot{M} \rangle \approx 5.4 \times 10^{-14}\ M_\odot/\mathrm{yr}$

$\dot{M}$ **anti-correlates** with $\langle V_{wind} \rangle$

$\Rightarrow$ geometrical effects dominate!